DOI 10.52209/2706-977X_2025_3_90 **IRSTI 81.09.03** **UDC 537.226**

Structures, Dielectric Constant, Impedance and Electrical Conductivity of Carbon/Cu_2O Nanowire (C/CONW) Composite Electrode Derived from Self-Adhesive Carbon Grain from Pre-Carbonized Date Palm leaves (Phoenix Dactylifera L.), Carbon Black and Cu Powder

Abbas Fatima Musbah[1]*, Abdelrahman Selma Elsheikh[2], Elsheikh Abdelrahman Abubaker[2]
[1]King Khalid University, Abha, Saudi Arabia
[2] NRC: National Research Centre, Sudan
*corresponding author

Abstract. Composite electrodes, especially carbon-metal oxide composites, hold promising potential in numerous industrial applications such as supercapacitors and electrochemical energy storage. This study focuses on developing high-performance composite electrodes utilizing pre-carbonized date palm leaves, carbon black and copper powder. The main objective of this research is to enhance the mechanical and electrical properties of composite electrodes while exploring the potential of agricultural waste utilization. The methodology involves ball-milling pre-carbonized date palm leaves (PCDPLs), followed by manual mixing with carbon black (CB) and copper (Cu) powder, pressing into pellets, and carbonization at 1000°C in a nitrogen environment. X-ray diffraction (XRD) analysis confirmed the polycrystalline structure of the composite electrode with EDXD confirming the presence of Cu_2O nanowires. Frequency-dependent dielectric parameters, impedance and electrical conductivity were analyzed utilizing the Cole–Cole plot in a range of (0-8) MHz. Results demonstrate improved crystallinity and performance of the composite electrodes, emphasizing the potential of utilizing agricultural waste for sustainable, high-performance electrode materials. This research highlights the importance of utilizing agricultural waste for developing advanced composite electrodes with enhanced performance capabilities, contributing to sustainable waste management and industrial applications in energy storage technologies.

Keywords: carbon/copper oxide composites, X-ray diffraction, pre-carbonized date palm leaves, Cu_2O nanowires, Cole-Cole plot.

Introduction

Composite electrodes or carbon-metal oxide electrodes are extensively developed employing distinct methodologies to improve industrial applications. For instance, carbon/metal oxide is a class of composite electrodes that has improved electrical properties and mechanical performances by incorporating a metal oxide compound. These types of composite electrodes have been utilized for transmission and distribution of electric power such as super capacitors [1] and electrochemical energy storage [2]. These are further developed by incorporating nanostructure fillers such as nanoparticles, nanowires and nanotube compounds to enhance the composite electrode mechanical performance and chemical stability [3]. It has also been revealed that the nano-structuring of the electrode materials has a positive effect on the electrode performance [4].

Currently, most commercial supercapacitor electrodes are manufactured from carbon due to its low cost, excellent corrosion resistance, superior cyclic stability and long service life, as the electrode does not undergo chemical alteration during charge/discharge cycles [5]. However, the maximum capacitance is restricted by the active electrode surface area and the pore size distribution [6].

Copper oxide (Cu2O) nanowires are widely utilized as p-type semiconductor compounds in numerous applications, including the degradation of methyl orange [7], super capacitors [8], heterojunction solar cells [9], biomedical fields [10] and surface coatings [11]. Depending on the preparation method and the proportions of constituents utilized, the copper oxide CuO phase may be accompanied by other complex structures, primarily Cu_2O and Cu4O3. Among these, CuO and Cu_2O are the most stable compounds. The synthesis method for Cu_2O nanostructure has been extensively reviewed in numerous researches which cover both physical and chemical methodologies [12-14].

Moreover, the carbon material in these types of composites can be prepared from numerous carbonaceous substances such as biomass material and agricultural waste material such as oil palm empty fruit bunch [15], olive stone [16], lignocellulose [17] and date palm leaves [18, 19]. In the present work, the raw carbon precursor is date palm leaves. Due to its high carbon content, low cost and low ash. Date palm leaves has been examined to produce solid carbon and activated carbon material with a high surface area and good electrical and mechanical properties [19]. Additionally, it has been revealed that pre-carbonized at low heat treatment and the milling process is very important to enhance the self-adhesive properties of the carbon produced.

Furthermore, the Cole–Cole plot proposed by Havriliak, Negami's and Debye is an analytical method utilized to characterize composite electrode. It illustrates the frequency dependence of impedance, dielectric parameters and conductivity. The Havriliak, Negami's and Debye explained the skewed and arcuate shape observed in graphical configuration of composite materials [20]. For instance, the dielectric constant (both real and imaginary parts) and the dielectric loss tangent are established methodologies for evaluating the conductivity behavior of electrode materials. A dielectric loss tangent greater than 1 indicates high conductivity whereas a tangent less than 1 indicates non-

conductive behavior [21]. It has been observed that the Cole–Cole plots of various electrodes, metal oxide and polymer materials tend to exhibit similar shapes [22].

Despite extensive development in the synthesis of composite electrodes, there remains an urgent need for optimizing the mechanical performance, chemical stability and electrical properties of these materials. This research emphasizes on the potential of incorporating nanostructure fillers to enhance electrode properties and explore the benefits of utilizing carbon derived from agricultural waste such as date palm leaves. The main objective is to synthesize composite electrode utilizing self-adhesive carbon grains from pre-carbonized date palm leaves, carbon black and copper powder. This research primarily focuses on the characterization of the crystalline structures and frequency-dependent properties such as dielectric constant, impedance and electrical conductivity of the composite electrode and to explore its potential applications thereby contributing to the field of advanced composite electrodes with improved performance capabilities.

The significance of this research lies in its innovative strategy of developing composite electrodes by utilizing self-adhesive carbon grains derived from pre-carbonized date palm leaves, carbon black and copper powder. By exploring the underutilized potential of agricultural waste, this research not only improves the mechanical and electrical properties of composite electrodes but also offers a sustainable solution to waste management. The incorporation of nanostructure fillers such as Cu_2O nanowires is expected to significantly improve the dielectric constant, impedance and electrical conductivity of the electrodes, thereby advancing their performance in industrial applications such as super capacitors and electrochemical energy storage [23]. This research also characterizes the frequency-dependent properties of these novel composite materials, providing valuable insights for further development and application in advanced material sciences.

1. Methodology

1.1 Pre-carbonized Date Palm leaves (PCDPLs)

The raw material that is the date palm leaves (Phoenix dactylifera L) were sectioned into small pieces and thoroughly washed with hot water. These pieces were subsequently dried at 100°C for two hours. The dried leaves then underwent pre-carbonization in a vacuum chamber at 280°C for 4 hours, leading to shrinkage and mass loss due to the expulsion of tars, oxygen, carbon monoxide and other volatiles components [24]. The pre-carbonized date palm leaves (PCDPL) were then ball-milled into fine carbon grain powder to enhance their self-adhesive properties.

1.2 Composite Electrode Preparation

The C/Cu_2O nanowire composite electrodes were synthesized by combining PCDPLs at concentrations of 50%, 60%, 70%, 80% and 90% with commercial carbon black at concentrations of 6%, 12%, 18%, 24% and 30% and copper powder (99.6% purity) at concentrations of 4%, 8%, 12%, 16% and 20%. The components were manually mixed and then stored in a plastic container. One gram of the resulting mixture was pressed into pellets by applying 12 metric tons of pressure without the addition of any binder. All grain pellets exhibited excellent self-adhesive properties before being carbonized at 1000°C in a nitrogen environment employing a multistep heating process, as described by [18].

Following carbonization, the composite electrode produced were thoroughly washed with hot distilled water to remove impurities until a pH of 6 was achieved, then dried in an oven at 100ºC for four hours. Measurement of the pellet dimension was carried out utilizing a micrometer screw gauge and the bulk density was determined by dividing the mass of the sample by its volume with results averaged over five replicates for each sample.

1.3 X-Ray Diffraction (XRD)

An X-ray diffraction (XRD) experiment was conducted on carbon composite pellets by utilizing Rigaku D/Max-X-ray diffractometer with Cu-Kα radiation. The scanning was conducted at a rate 5 seconds per 0.1° step size, covering a diffraction angle (2θ) range from 20° to 70°.

1.4 Energy Dispersions X-ray Diffraction (EDXD)

Energy dispersion X-ray diffraction (EDXD) was employed on selected sample to identify the structure of Cu_2O nanowire.

1.5 Dielectric Constants

The frequency dependent dielectric parameters, specifically the Real part (*Er*) and imaginary part (*Ei*) were analyzed utilizing the Cole–Cole plot. The real and the imaginary parts were determined as stated by [21, 25]

$$Er(\omega) = E_o + r^{\frac{-A}{2}}(E_o - E_\infty)\, cosA\theta \quad (1)$$

$$Ei(\omega) = r^{\frac{-A}{2}}(E_o - E_\infty)\, SinA\theta \quad (2)$$

$$TanA\theta = \frac{Ei(\omega)}{Er(\omega) - E_o} \quad (3)$$

$$\text{Phase } (\theta) = \frac{1}{A} Tan^{-1}\left(\frac{Ei(\omega)}{(Er(\omega) - Eo)}\right) \quad (4)$$

$$\text{Dielectric loss Tangent} = \frac{Ei(\omega)}{Er(\omega)} \quad (5)$$

where r is the constant and A is the angular frequency.

1.6 Impedance (Z)

The frequency dependence of impedance and conductivity both the real part and the imaginary part was measured employing an e-Agilent E4980A precision LRC meter (inductance [L], capacitance [C], and resistance [R]) cell devise. This analysis utilized the Cole-Cole plot to refer to Debye behaviours as done in previous researches [21, 26]. The measurements were performed utilizing option 001 (DC Measurements) by applying voltages from 0 to 5 V with a frequency range of 103MHz to 8x 10^5 Hz to characterize the impedance and conductivity behavior of the composite electrode. Impedance which depends on the frequency (ω) of the source, is described as the combination of the real part (Z') and the imaginary part (Z") as stated by [27].

$$Z = Z' + iZ'' \quad (6)$$

$$Z' = \frac{R_p}{1+(\omega R_p C_p)^2} \quad (7)$$

$$Z'' = \frac{\omega R_p^2 C_p}{1+(\omega R_p C_p)^2} \quad (8)$$

The value of the C_p can be given from equations (2) and (3) at medium and lower frequency range as

$$C_p = \frac{Z''}{Z' R_p} \quad (9)$$

1.7 Electrical Conductivity (EC)

The frequency-dependent analysis of conductivity, including the real part (EC(r)) and imaginary part (EC(i)) was conducted utilizing the Cole-Cole plot to refer to Debye behaviors, following the approach outlined by [21]. An electrical component with option 001 (DC Measurements) was employed, applying voltages ranging from 0–5 volts and frequencies ranging from 0 MHz –6.5 MHz to analyze the conductivity behavior of the produced electrode. The AC conductivity is defined as

$$EC(AC) = Ec(DC) + A(\omega)^s \quad (10)$$

where DC is the direct current, $\omega = 2\pi f$, f is the frequency and A is a constant.

2.Result and Discussion

2.1 Composite Electrode Properties

Table 1 demonstrates data on the average weight and bulk density of composite electrode (C/Cu_2O) nanowire. The bulk density exhibits a slight increase from 1.303 g/cm^3 to 2.26 g/cm^3 with the augmentation CB+Cu % content. The density of the carbon composite pellets is approximately 50% of that of pure-graphite structure and falls within the range of densities for carbon filament electrodes (1.77 g/cm^3) and glassy carbon (Sigradur K) (1.540 g/cm^3), indicating that the composite has achieved substantial density. Additionally, the table also reveals that the yield of the composite electrode improves with increasing CB+Cu % content. This improvement is attributed to a reduction in non-carbon content and volatile components which contributes to the enhanced bulk density of the product.

Table 2. The raw composition concentrations data before and after carbonization

Raw Data Before Carbonization				Data After Carbonization		
PCDPLs %	CB %	Cu %	Weigh	Weight	Electrode	Black Density
			(g)	(g)	Yield	(g/cm^3)
90%	6%	4%	1.00	0.48±0.01	48%	1.30±0.03
80%	12%	8%	1.00	0.53±0.03	53%	1.38±0.02
70%	18%	12%	1.00	0.56±0.00	56%	1.86±0.05
60%	24%	16%	1.00	0.59±0.01	59%	2.02±0.11
50%	30%	20%	1.00	0.62±0.01	62%	2.25±0.01
Carbon filament electrode	-	-	-	-	-	1.77
Graphite	-	-	-	-	-	2.26
Sigradur K	-	-	-	-	-	1.540
			(g)	(g)	Yield	(g/cm^3)
90%	6%	4%	1.00	0.48±0.01	48%	1.30±0.03
80%	12%	8%	1.00	0.53±0.03	53%	1.38±0.02
70%	18%	12%	1.00	0.56±0.00	56%	1.86±0.05
60%	24%	16%	1.00	0.59±0.01	59%	2.02±0.11
50%	30%	20%	1.00	0.62±0.01	62%	2.25±0.01
Carbon filament electrode	-	-	-	-	-	1.77
Graphite	-	-	-	-	-	2.26
Sigradur K	-	-	-	-	-	1.540

2.2 X-ray Diffraction

Figure 1 illustrates the X-ray diffraction pattern for composite electrode pellets exhibiting strong peaks at reflection planes (002), (110), (111), (100), (200) and (111) corresponding to diffraction angles (2θ) of 25.9°, 28.7°, 36.4, 39.69°, 43.9, 50°.32 and 53.25° respectively. This pattern indicates a polycrystalline structure. It is evidently proven from figure 1 that the composite electrode produced enhances the crystalline structure as distinguished by three prominent sharp peaks at (002), (100) and (111) characteristic of a graphitic-like structure. Additionally, strong diffraction peaks (110), (111), (200) and (211) represent the dominant structure of Cu_2O in the composite.

Moreover, the X-ray spectrum analysis indicates that an increase in the percentage of (CB+Cu) % content leads to the enhancement in the crystalline structure of the produced composite electrode. This effect is especially pronounced in the composite electrode sample prepared with a 50% concentration which exhibits a structure of pure-graphitic as evidenced by the X-ray diffraction spectrum depicted in Figure 1. Furthermore, these findings correspond with the bulk density measurement as demonstrated in Table 1, which shows equivalence to that of pure graphite.

These observations support the concept that the combination of (Cu+ CB) with PCDPLs promotes a more graphitic structure, reducing the graphitization temperature up to 1000^{o}C by employing multiple heating profiles in nitrogen environments. This reduction in graphitization temperature is expected to yield economic benefits and provides an alternative approach to minimize graphite production costs.

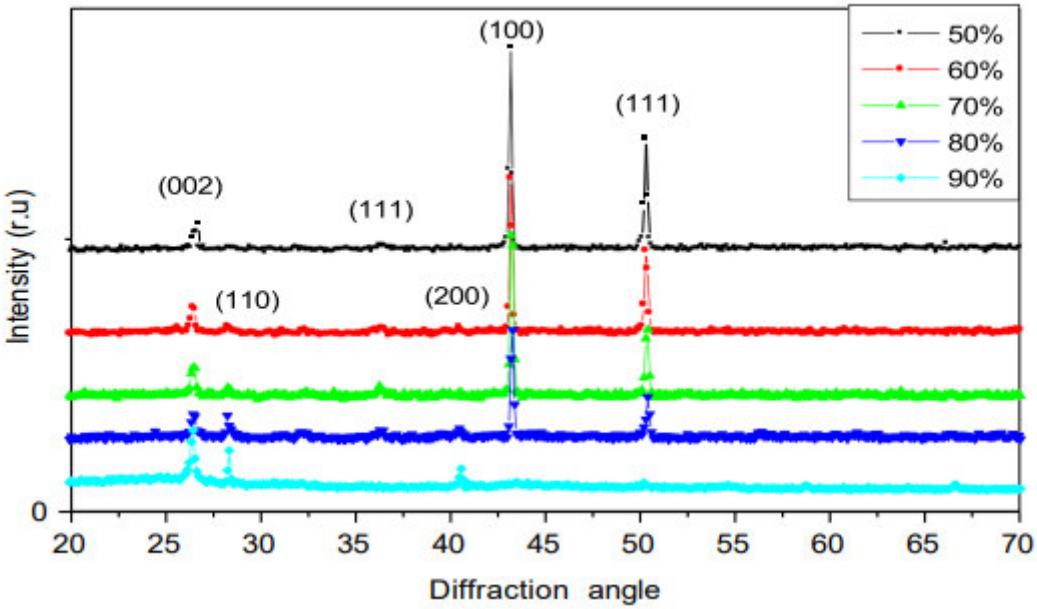

Fig. 8. - X-ray diffraction profiles of the C/Cu_2O nanowire composite electrode.

2.3 EDXD

Figure 2 illustrates the visual representation of the EDXD electron image exhibiting a specific composite electrode treated with 70% PCDPLs. It reveals the vertical growth of Cu_2O nanowires on the Cu/Cu_2O cluster substrate synthesized through a pyrolysis mechanism, exhibiting varying orientations.

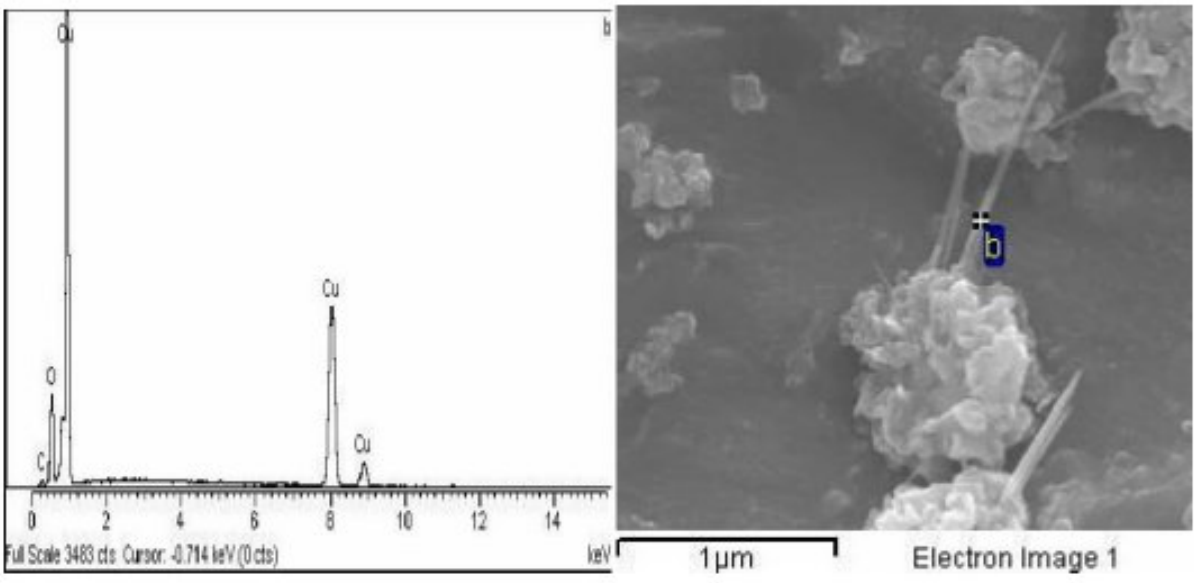

Fig. 2. - EDXD electron image of the selected composite electrode

2.4 Impedance

The widely recognized Cole–Cole plot originally proposed by Havriliak and Negami's through analytical methods explained the graphical configuration and arcuate shape observed in the medium and low frequency range (103MHz – 8x105Hz) of the composite electrode. However, the presence of a semicircular sketch was not detected within this frequency range as illustrated in Figure 3. It is expected that the frequency ranges utilized are insufficient to fully capture the threshold dominance of the Havriliak and Negami's analytical behavior.

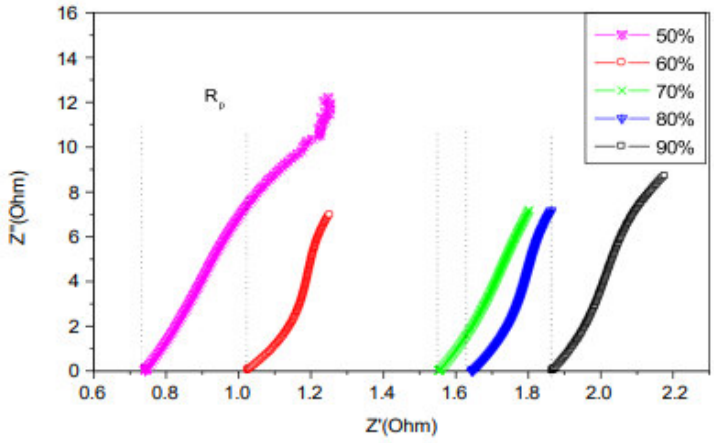

Fig. 9. - Cole-Cole Plots illustrating the frequency-dependent impedance, with the imaginary part (Z") plotted against the real part (Z') for composite samples ranging in concentration from 50% to 90%.

Additionally, the impedance bridge data demonstrated in Table 2 highlights the values of Rp (polarization resistance) and the maximum Z" (imaginary part) and Z' (real part) at medium and lower frequencies. The data from the table 2 also reveals that the Z" value for the 90% concentration and Z' value for the 50% concentration are higher as compared to other electrode compositions, suggesting an enhancement in Z' with an increase in (CB+Cu) % content.

Table 3. Impedance results plotted in a Cole-Cole plot as a function of frequency

Composite Electrode Cell	Rp (Ohm)	Z''(max) (Ohm)	Z'(max) (Ohm)
90%	0.735	12.30	1.250
80%	1.021	7.00	1.250
70%	1.550	7.33	1.800
60%	1.630	7.19	1.870
50%	1.860	8.80	2.175

Furthermore, it is evident from the data that the Cole–Cole plots observed in numerous carbon electrodes and metal oxide exhibited that all these plots have approximately similar shape as reported by [28].

2.5 Electrical Conductivity (EC)

Figures 4 and 5 illustrates the frequency-dependent variation of electrical conductivity represented by the real part (EC(r)) and imaginary part (EC(i)) respectively, composite electrode samples treated with different percentages of PCDPLs (50%, 60%, 70% and 80%) (298 K). Notably, the real part exhibits a marked increase at lower frequencies followed by a decrease at higher frequencies, indicating a characteristic behavior. The intercept on the y-axis represents the DC resistance as noted by [29]. On the Contrary, the imaginary part exhibits a significant increase at lower frequencies and a subsequent decrease at higher frequencies.

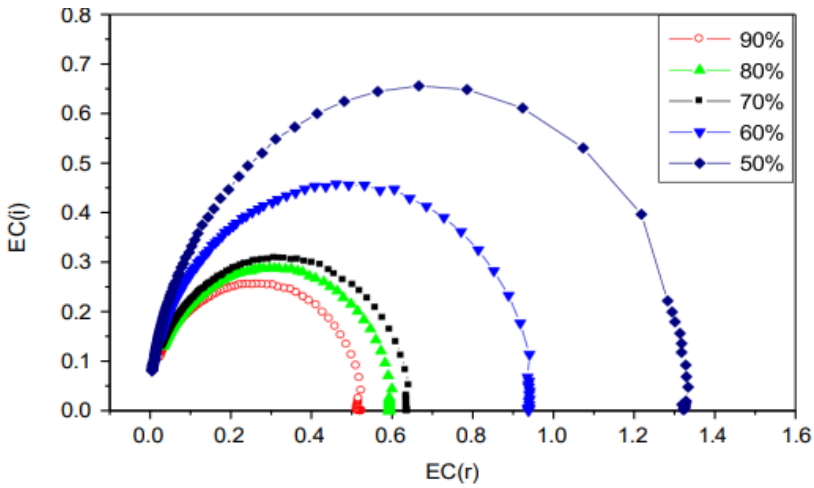

Fig. 10. - The Cole-Cole plots of frequency dependence impedance (imaginary part Z" versus the real part Z') for composite samples treated with varying percentages of PCDPL, ranging from 50% to 90%.

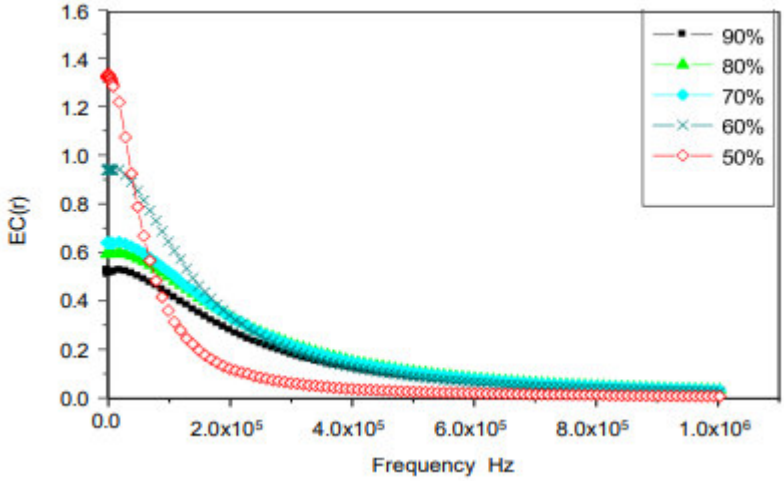

Fig. 11. - Frequency-dependent variation of electrical conductivity represented by the real part (EC(r)) of composite electrode samples treated with varying percentages of PCDPL, ranging from 50% to 90%.

Additionally, the Cole-Cole graphical plot of the imaginary part (EC(i)) is plotted against the real part at (EC(r)) as a function of frequency [30]. This plot reveals the semi-circular patterns with a narrow threshold range from 0 to 1.32 as observed in Figure 6 and demonstrated in Table 2. Figure 6 explains the theoretical behavior predicted by the Debye method as discussed by [21]. Furthermore, it is observed that the semicircular sketch patterns increase with higher percentages of (CB+Cu), indicating a rise in electrical conductivity with increasing (CB+Cu) content although the conductivity values remain relatively low.

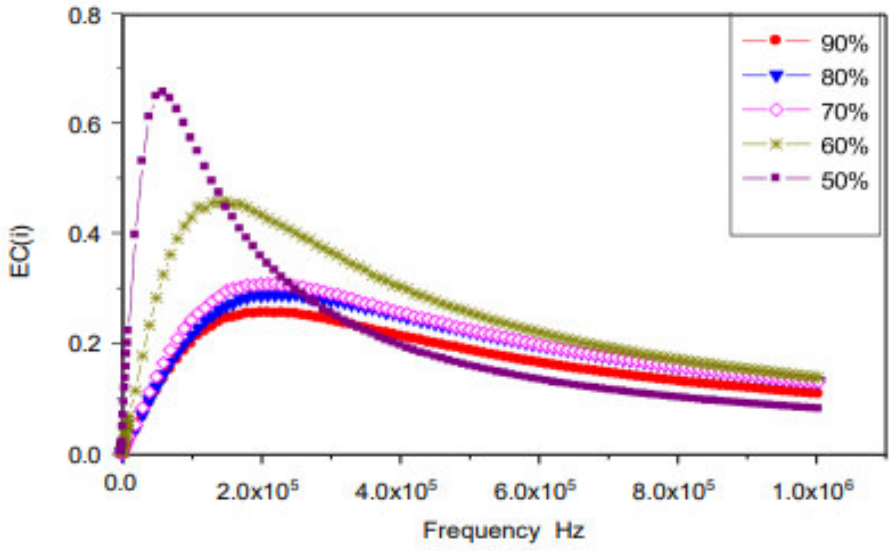

Fig. 12. - Frequency-dependent variation of electrical conductivity represented by the imaginary part (EC(i)) of composite electrode samples treated with varying percentages of PCDPL, ranging from 50% to 90%.

These effects are expected to the vertical growth of Cu_2O nanowires in varying orientations on the surface of the composite electrode, as illustrated in Figure 2. This vertical growth is expected to hinder the transfer of mobility carriers, consequently reducing the electrical conductivity behavior of the produced composite electrode, as suggested by [26]. Most Probably, this behavior is due to the addition of CB and Cu as rigid fillers to the PCDPLs, leading to enhanced electrical properties of the composite product and also by enhancing occupational mobility carrier in the electrode contact points.

Moreover, table 3 demonstrates the relationship between the percentage of composite electrode cell and the Cole-Cole plot of conductivity behavior as a function of frequency. It reveals the range of frequencies over which the imaginary electrical conductivity (EC(i)) increases then decreases for different composite electrode cell percentages. The table suggests that the frequency range over which this behavior is observed increases as the percentage of composite electrode cell increases.

Table 4. Cole-Cole plot of Conductivity Behavior as a Function of Frequency

Composite electrode cell	Semi-circular sketch dominos (EC (r))	EC(i) max
90%	(0 - 0.520)	0.255
80%	(0 - 0.591)	0.287
70%	(0 - 0.642)	0.303
60%	(0 - 0.938)	0.453
50%	(0 - 1.32)	0.644

Conclusion

A Carbon/Cu_2O nanowire composite electrode has been successfully developed utilizing pre-carbonized date palm leaves, carbon black and Cu powder, exhibiting improved mechanical and electrical properties. XRD analysis revealed that all CCOC pellets possess a polycrystalline structure while EDXD results confirmed the Cu_2O structure as nanowire. The combination of three materials, i.e. biomass PCDPLs + CB and Cu results in nanoparticle-composite carbon with significantly improved crystallinity. The incorporation of Cu_2O nanowires enhanced the dielectric constant, impedance and conductivity. Cole-Cole plots revealed consistent frequency-dependent behavior across distinct composite compositions. This research emphasizes on the potential of utilizing agricultural waste for developing advanced, high-performance composite electrodes for industrial applications, particularly in supercapacitors and electrochemical energy storage.

The study's limitations include a narrow frequency range for impedance analysis, potentially insufficient to fully capture the Havriliak and Negami's behavior and the relatively low conductivity values due to the vertical growth of Cu_2O nanowires may hinder carrier mobility in the composite electrode. Additionally, the research also does not extensively explore the benefits of other metal oxides compared to Cu2O. Furthermore, the specific impact of each constituent (PCDPLs, CB, Cu) on the mechanical and electrical properties was not fully studied.

This study opens pathways for broader applications in renewable energy technologies, such as solar cells and fuel cells. The sustainable approach of utilizing agricultural waste could inspire further researches into other biomass-derived materials, promoting circular economy principles and cost-effective electrode manufacturing. Additionally, the improved dielectric properties and impedance behaviors of these composites may lead to advancements in electronic devices and sensors, providing a versatile platform for future innovations in various high-performance technological sectors.

Data Availability Statement: The datasets generated and/or analyzed during the current study are available from the corresponding author, Fatima Musbah Abbas, upon reasonable request.

Competing Interests: The authors have no relevant financial or non-financial interests to disclose.

Funding: The authors declare that no funds, grants, or other support were received during the preparation of this manuscript.

Author Contributions: All authors contributed to the study conception and design. Material preparation, data collection and analysis were performed by [Fatima Musbah Abbas], [Selma Elsheikh Abdelrahman] and [Abubaker Elsheikh Abdelrahman]. The first draft of the manuscript was written by [Fatima Musbah Abbas] and all authors commented on previous versions of the manuscript. All authors read and approved the final manuscript.

Acknowledgements: The authors extend their appreciation to Deanship of Scientific Research at King Khalid University for funding this research through General Research Project under grant number (RGP.1/127/44-1444).

References

[1] S. Saini, P. Chand, and A. Joshi, "Biomass derived carbon for supercapacitor applications," Journal of Energy Storage, vol. 39, p. 102646, 2021.

[2] R. Liu et al., "Carbon coating on metal oxide materials for electrochemical energy storage," Nanotechnology, vol. 32, no. 50, p. 502004, 2021.

[3] A. Barra, C. Nunes, E. Ruiz-Hitzky, and P. Ferreira, "Green carbon nanostructures for functional composite materials," International Journal of Molecular Sciences, vol. 23, no. 3, p. 1848, 2022.

[4] R. Xu et al., "Well-defined nanostructures for electrochemical energy conversion and storage," Advanced Energy Materials, vol. 11, no. 15, p. 2001537, 2021.

[5] Y. Wang et al., "Recent progress in carbon-based materials for supercapacitor electrodes: a review," Journal of Materials Science, vol. 56, pp. 173-200, 2021.

[6] A. Elmouwahidi, E. Bailón-García, J. Castelo-Quibén, A. Pérez-Cadenas, F. Maldonado-Hódar, and F. Carrasco-Marín, "Carbon–TiO 2 composites as high-performance supercapacitor electrodes: synergistic effect between carbon and metal oxide phases," Journal of Materials Chemistry A, vol. 6, no. 2, pp. 633-644, 2018.

[7] Z. Xie et al., "Effect of impurity in Cu 2 O nanowires on the degradation of methyl orange," Journal of Materials Science: Materials in Electronics, vol. 31, pp. 3817-3824, 2020.

[8] D. Majumdar and S. Ghosh, "Recent advancements of copper oxide based nanomaterials for supercapacitor applications," Journal of Energy Storage, vol. 34, p. 101995, 2021.
[9] C. Dumitru, V.-F. Muscurel, and L. Fara, "Cu_2O layer analysis and optimization based on a metal-oxide tandem heterojunction solar cell," Materials Today: Proceedings, vol. 5, no. 8, pp. 15895-15901, 2018.
[10] N. Verma and N. Kumar, Synthesis and biomedical applications of copper oxide nanoparticles: an expanding horizon," ACS biomaterials science & engineering, vol. 5, no. 3, pp. 1170-1188, 2019.
[11] S. Masroor, "Basics of metal oxides: properties and applications," Inorganic Anticorrosive Materials, pp. 85-94, 2022.
[12] T. H. Tran et al., Effect of annealing temperature on morphology and structure of CuO nanowires grown by thermal oxidation method, Journal of Crystal Growth, vol. 505, pp. 33-37, 2019.
[13] Z. Starowicz et al., Materials studies of copper oxides obtained by low temperature oxidation of copper sheets," Materials Science in Semiconductor Processing, vol. 121, p. 105368, 2021.
[14] M. Košiček, J. Zavašnik, O. Baranov, B. Šetina Batič, and U. Cvelbar, "Understanding the growth of copper oxide nanowires and layers by thermal oxidation over a broad temperature range at atmospheric pressure," Crystal Growth & Design, vol. 22, no. 11, pp. 6656-6666, 2022.
[15] M. Ikhsan and R. Ramli, "Measurements and analysis of crystal structures of activated carbon of empty fruit bunch from oil palm biomass waste," in Journal of Physics: Conference Series, 2020, vol. 1528, no. 1: IOP Publishing, p. 012031.
[16] P. Ibeh, F. García-Mateos, J. Rosas, J. Rodríguez-Mirasol, and T. Cordero, "Activated carbon monoliths from lignocellulosic biomass waste for electrochemical applications," Journal of the Taiwan Institute of Chemical Engineers, vol. 97, pp. 480-488, 2019.
[17] V. Dhyani and T. Bhaskar, "A comprehensive review on the pyrolysis of lignocellulosic biomass," Renewable energy, vol. 129, pp. 695-716, 2018.
[18] F. M. Abbas, Z. A. Al Ahmad, R. O. E. Elgezouly, and A. E. Abdelrahman, "Characterization of carbon pellets prepared from date palm leaves (Phoenix dactylifera L.) by compression pressure: X-ray diffraction measurements and applications," 2022.
[19] A. E. Abdelrahman, F. M. Abbas, and A. K. Arof, "Crystallite Parameters, Amorphous Contents and Surface Functional Groups, Contents of Activated Carbon Prepared from KOH Treated Pre-Carbonized Date Palm Leaves (Phoenix dactylifera L.)," 2023.
[20] S. Bhattacharjee, A. Banerjee, N. Mazumder, K. Chanda, S. Sarkar, and K. K. Chattopadhyay, "Negative capacitance switching in size-modulated Fe 3 O 4 nanoparticles with spontaneous non-stoichiometry: confronting its generalized origin in non-ferroelectric materials," Nanoscale, vol. 12, no. 3, pp. 1528-1540, 2020.
[21] R. Han, Y. Liu, J. Shi, G.-X. Chen, and Q. Li, "Enhanced dielectric properties and breakdown strength of polymer/carbon nanotube composites by coating an SrTiO3 layer," e-Polymers, vol. 21, no. 1, pp. 272-278, 2021.
[22] G. A. Khouqeer, B. A. El-Badry, and M. Zaki, "Improvement of the optical properties, dielectric behaviors and Cole-Cole plot of gamma-irradiated polyvinyl alcohol filled by nanostructured aluminum metal oxide," Journal of Radiation Research and Applied Sciences, vol. 17, no. 2, p. 100871, 2024.
[23] M. Harilal et al., "Environment-modulated crystallization of Cu_2O and CuO nanowires by electrospinning and their charge storage properties," Langmuir, vol. 34, no. 5, pp. 1873-1882, 2018.
[24] V. D. Vaibhav Dhyani and T. B. Thallada Bhaskar, "A comprehensive review on the pyrolysis of lignocellulosic biomass," 2018.
[25] Wilczyński K., Wróblewska A., Daniszewska A., Krupka J., Mrozowski M., Zdrojek M. Modulation of dielectric properties in low-loss polypropylene-based composites at GHz frequencies: theory and experiment //Scientific Reports, vol. 12, no. 1, p. 13104, 2022.
[26] Aguilo-Aguayo N., Drozdzik T., Bechtold T. Impedance analysis of electrodes made of continuous carbon filaments in a 20 cm^2 redox flow cell //Journal of Electroanalytical Chemistry, vol. 926, p. 116954, 2022.
[27] Demirezen S., Yerişkin S. A. Frequency and voltage-dependent dielectric spectroscopy characterization of Al/(Coumarin-PVA)/p-Si structures // Journal of Materials Science: Materials in Electronics, vol. 32, pp. 25339-25349, 2021.
[28] Samatha K., Vijeth H., Sagar R. Electrical and electrochemical properties of nanostructured Ni and Zn substituted Co_3O_4 spinels for thermistors and supercapacitor applications //Journal of Energy Storage, vol. 52, p. 104871, 2022.
[29] Jiang Y., Huang J., Ji H., Wang B., Huang Z., Soleimani M. Study on dual-frequency imaging of capacitively coupled electrical impedance tomography: Frequency optimization //IEEE Transactions on Instrumentation and Measurement, vol. 71, pp. 1-18, 2022.
[30] Tan C. Y., Farhana N., Saidi N. M., Ramesh S., Ramesh K. Conductivity, dielectric studies and structural properties of P (VA-co-PE) and its application in dye sensitized solar cell //Organic Electronics, vol. 56, pp. 116-124, 2018.

Information of the authors

Abbas Fatima Musbah, PhD, professor, King Khalid University, College of Science and Art, Dhahran Aljanoub
e-mail: FatimaM.Abbas1@researchergroup.co

Abdelrahman Selma Elsheikh, PhD, associate professor, National Research Centre
e-mail: Selma_111@yahoo.com

Elsheikh Abdelrahman Abubaker, PhD, associate professor, National Research Centre
e-mail: abuelsheikh76@gmail.com